Ultrafast rainbow: tunable ultrashort pulses from a solid-state kilohertz system

Kent R. Wilson and Vladislav V. Yakovlev

Department of Chemistry and Biochemistry, University of California, San Diego, La Jolla, California 92093-0339

Received February 13, 1996; revised manuscript received July 11, 1996

Two stages of type II optical parametric amplification of a white-light continuum are used for efficient generation of ultrashort (30–50-fs) pulses at kilohertz repetition rates. Various nonlinear techniques can be used to cover the range from 12 μm to 280 nm. The amplitude and the phase of the generated UV pulses are characterized by use of frequency-resolved optical gating. © 1997 Optical Society of America
[S0740-3224(97)02602-7]

For the past few years, optical parametric generators and amplifiers have proved to be a convenient way to extend the tunability of femtosecond lasers in compact all-solid-state systems.[1–7] In these systems a strong femtosecond pulse is used to amplify a portion of a white-light continuum or parametric fluorescence. The amplified wavelength depends on the phase-matching angle of the nonlinear crystal, and thus tunability can easily be accomplished. 100-fs femtosecond pulses can now be routinely generated by use of either the fundamental or the second harmonic of Ti:sapphire as the pump wavelength. Shorter pulses have been achieved only with the optical parametric amplification (OPA) of a white-light continuum followed by pulse compression.[3,4,7] Inasmuch as we use these pulses in quantum control experiments,[8] it is important to generate short pulses in the IR and the UV ranges where most molecular vibrational and electronic absorption occurs.

In the present study we use type II phase matching to improve the performance of the white-light OPA developed earlier[3] to achieve higher conversion efficiencies, more control of the amplified bandwidth, higher pulse energies, and broader tunability. We apply frequency-resolved optical gating[9,10] (FROG) to characterize the UV pulses and compress them to their transform limit.

Type II phase matching, $e(\text{pump}) \rightarrow e(\text{idler}) + o(\text{signal})$, has the advantage of providing a way to separate the signal and the idler waves, because they have different polarizations. This is especially important when one is operating near the degeneracy point where these wavelengths are close to each other. A second significant feature of type II phase matching in β-barium borate (BBO) crystals is that the relative (with respect to the pump) velocity of the signal wave is the opposite of that of the idler wave in most of the tuning range of the pump (see Fig. 1). This means that the energy flow happens mostly in the direction from pump to signal and idler, resulting in higher conversion efficiency of the parametric interaction. Simulations[11,12] predict exponential growth of the signal and the idler, even if the crystal length exceeds the separation length of the pump and the signal waves because of group-velocity dispersion (typically 2 mm for 790-nm pumping). The third feature of type II phase matching in BBO pumped by a Ti:sapphire fundamental that makes it more attractive than type I phase matching is that the amplified bandwidth[12] is almost independent of the wavelength of the signal (see Fig. 2). This results in better control of the bandwidth of the amplified pulses. A drawback of type II interaction is lower effective nonlinearity, so higher pump intensity is required for the same gain.

Our pump consists of a kilohertz chirped-pulse amplification Ti:sapphire system[13] delivering ~500 μJ of energy in 50 fs, at a center wavelength of 790 nm. Of this energy, ~2 μJ is used to generate a single-filament white-light continuum in a 2-mm-thick sapphire (see Fig. 3). 50 μJ of energy is downcollimated to create an intensity of ~50 GW/cm^2 on the entrance of the first 3- (or 5-) mm-long BBO Type II ($\Theta = 28°$) crystal. The surfaces of the crystals are antireflection coated for 800 and 1200 nm. One can adjust the intensity of the pump pulse by slightly changing one of the collimating lenses. The best results are achieved when this intensity is adjusted such that the parametric fluorescence mixed with the 790-nm light produces visible light seen by eye and the mode of the white-light continuum is matched to the pump beam diameter. In this case, when the time delay between the pump and the amplified portion of the white-light continuum is properly adjusted, the parametric fluorescence disappears, and as much as 6 μJ of amplified IR light can be detected. The only significant difference in performance between 3- or 5-mm-long BBO crystals is a broader amplification bandwidth in the case of the 3-mm crystal and a smaller intensity required for generation of the same gain in the case of the 5-mm-long crystal. This means that the effects of group-velocity mismatch between signal and pump are not so critical as in the case of type I phase matching.[3] The second stage of amplification consists of an identical BBO crystal pumped with ~450 μJ of 790-nm light and run in the saturation regime, resulting in stable amplification. We measure as much as 200 μJ of amplified light directly after the nonlinear crystal, corresponding to 45% energy-conversion efficiency. Wavelength tuning is usually done in the following way. First

0740-3224/97/020444-05$10.00

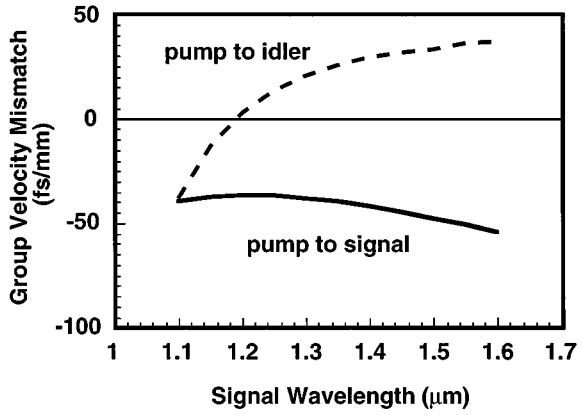

Fig. 1. Calculated group-velocity mismatch between pump and signal waves (solid curve) and pump and idler waves (dashed curve) for the 790-nm pump wavelength.

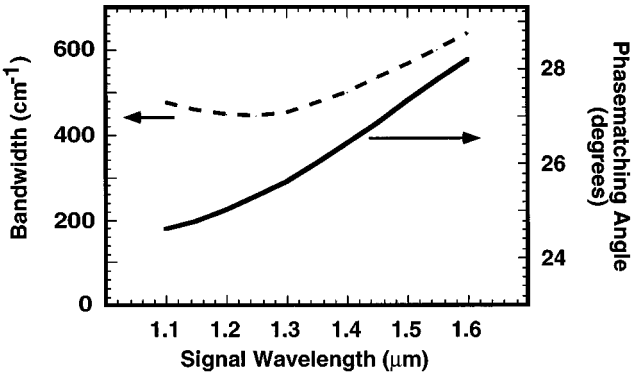

Fig. 2. Calculated external phase-matching angle (solid curve) and amplified bandwidth (dashed curve) for a 3-mm-long BBO crystal with a pump intensity of ~100 GW/cm^2.

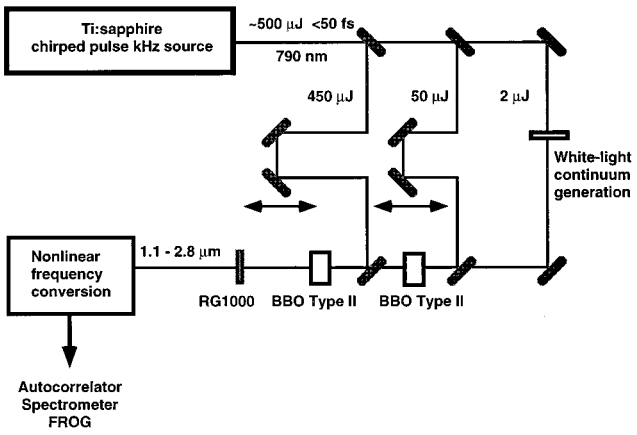

Fig. 3. Schematic of the experimental apparatus.

the nonlinear crystal in the first stage of amplification is angle tuned; then the delay of its pump is adjusted to maximize the amplified IR light. After that, the output power is optimized by iterative tuning of the second-stage phase-matching angle and fine adjustment of its pump delay. A RG1000 Schott glass filter (Fig. 3; more than 90% transmission for wavelengths longer than 1.1 μm) is usually used to block the residual pump beam after the final amplifier.

Following the scheme described in Ref. 3, we are able to generate as much as 20 μJ of tunable visible light by second-harmonic generation from the signal wave in a 250-μm-thick BBO crystal. The bandwidth of these visible pulses does not change dramatically as the wavelength is tuned from 800 to 550 nm and is of the order of 300–450 cm^{-1}, corresponding to transform-limited pulses of 30 fs or less. By independently adjusting the OPA crystals as was suggested in Ref. 3 and later demonstrated by Sosnowski *et al.*,[7] we are able to generate even

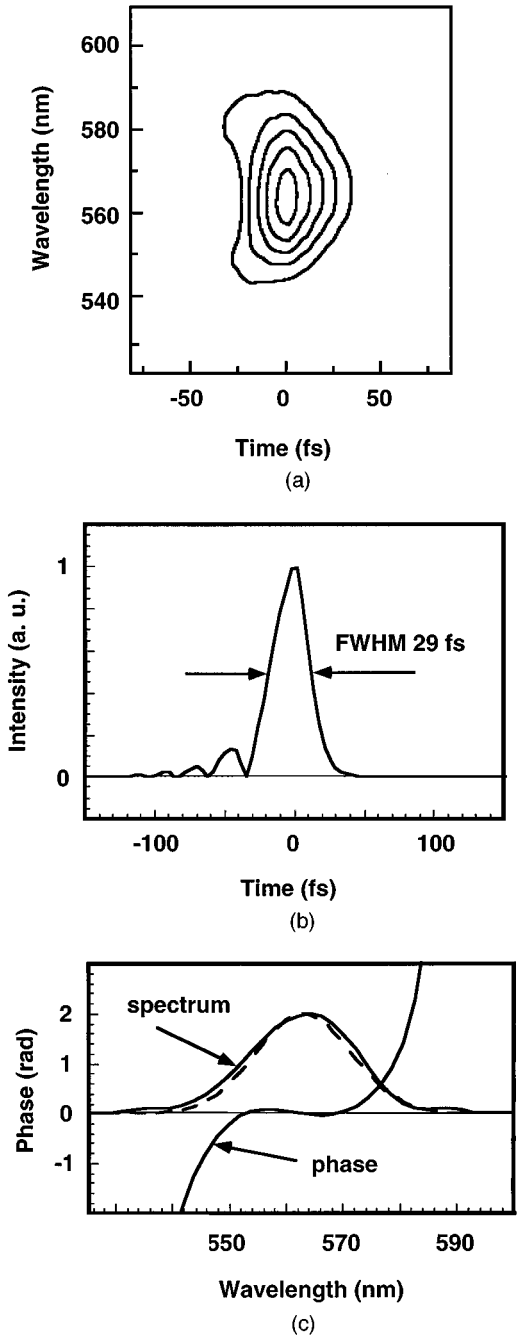

Fig. 4. (a) FROG measurement of compressed pulses at 560 nm. (b) Reconstructed temporal pulse shape corresponding to a pulse duration of 29 fs. (c) Reconstructed (solid curve) spectrum and phase of the pulses. The experimentally measured spectrum is shown as a dashed curve.

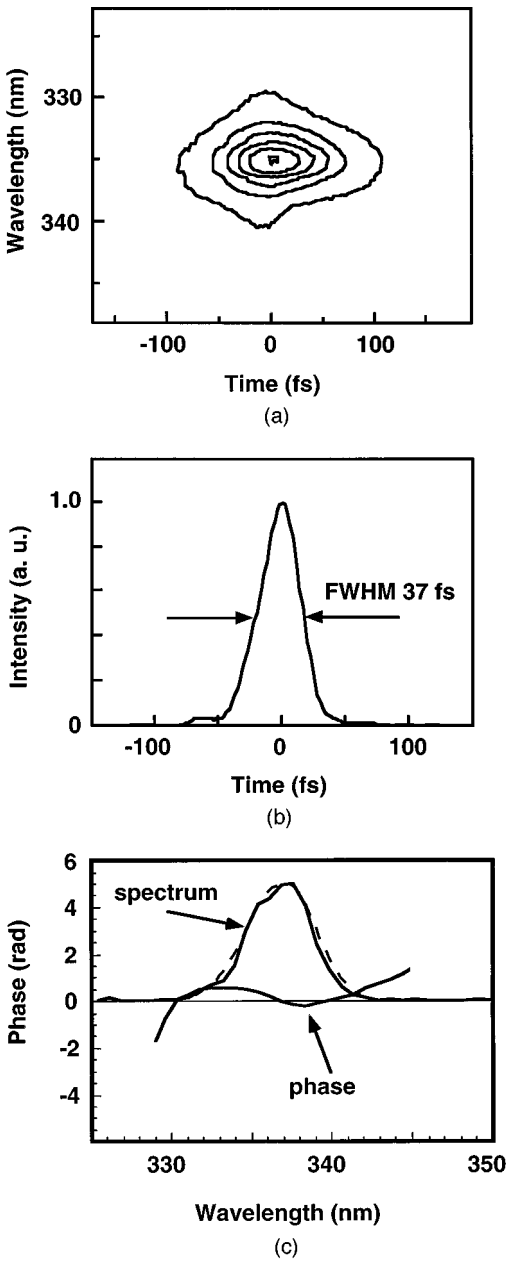

Fig. 5. (a) FROG measurement of compressed pulses at 335 nm. (b) Reconstructed temporal pulse shape, corresponding to a pulse duration of 37 fs. (c) Reconstructed (solid curve) spectrum and phase of the pulses. The experimentally measured spectrum is shown as a dashed curve.

larger bandwidths that usually exhibit a flat-topped or double-peaked structure. Such spectra can lead to pulses shorter than 20 fs.

We use a prism compressor consisting of LaK31 prisms to compress the pulses and precompensate for the material in our FROG setup.[9,10] We use the polarization FROG technique to discover how best to compress the pulses and to analyze the residual chirp. Special care is taken to ensure the absence of spatial chirp on the beam. By adjusting the amount of prism insertion material, we are able to generate pulses of the order of 30 fs. A typical FROG measurement of such a visible pulse is shown in Fig. 4(a) and corresponds to a deconvolved pulse duration of 29 fs [Fig. 4(b)] with significant uncompensated quadratic chirp accumulated in the prism compressor [Fig. 4(c)].

We produce tunable UV pulses by generating the second harmonics of the visible pulses. Another approach is to mix the residual 790-nm wave with the visible pulse, which is easier to accomplish because the group-velocity dispersion is less but the wavelength tunability is more limited. We find that type II phase matching in BBO is most appropriate for second-harmonic generation because the acceptance bandwidth is three times larger than in the case of type I BBO and 30% more than in the case of type I lithium triborate. This is confirmed by actual measurements of the bandwidth of the generated second harmonic in these crystals.

We are able to generate more than 1 μJ of tunable UV light by direct doubling of 10 μJ of the visible light in a

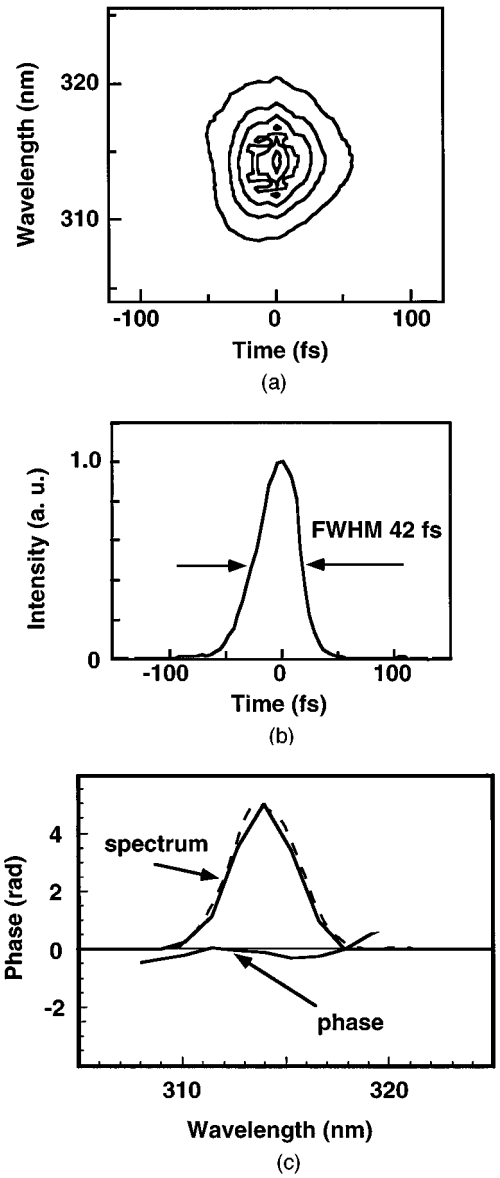

Fig. 6. (a) FROG measurement of a compressed pulse at 314 nm. (b) Reconstructed temporal pulse shape, corresponding to a pulse duration of 42 fs. (c) Reconstructed (solid curve) spectrum and phase of the pulses. The experimentally measured spectrum is shown as a dashed curve.

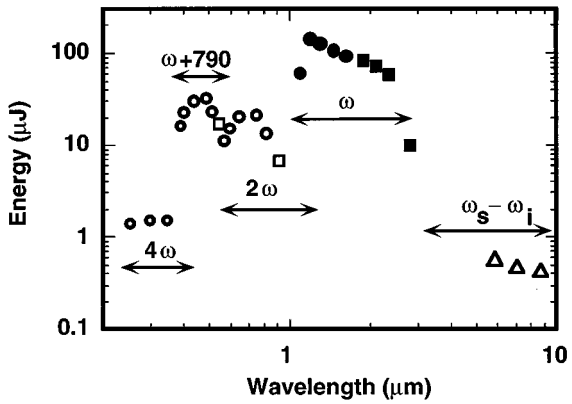

Fig. 7. Filled circles and filled squares show the measured energy of the amplified signal and idler waves, respectively. Open circles and open squares show the measured energy of the pulses generated by different nonlinear processes. 2ω, second harmonic of the signal (circles) and the idler (squares) (type I phase matching in 0.25-mm-thick BBO); $\omega + 790$: sum-frequency generation from the residual 790 nm and signal (type II phase matching in 0.2-mm-thick BBO); 4ω, fourth harmonic ($2\omega + 2\omega$) of the signal pulse (type II in 0.2-mm-thick BBO); open triangles, $\omega_S - \omega_i$: difference frequency generation (Type I in 1-mm-thick $AgGaS_2$).

250-μm BBO crystal (type II, $\Theta = 40°$). The spectrum of this pulse has a bandwidth of 400 cm^{-1}, corresponding approximately to a 30-fs pulse, assuming a Gaussian pulse shape. In fact, we find that the bandwidth is always limited by the acceptance bandwidth of the nonlinear crystal; thus thinner crystals should result in broader bandwidths and hence in shorter pulses. This also permits the achievement of a limited tunability of the second-harmonic pulse for a fixed wavelength of the fundamental. To compress such UV pulses we use a fused-silica prism compressor. The FROG measurement of compressed pulses centered at 335 nm is shown in Fig. 5(a) and corresponds to a pulse duration of 37 fs [Fig. 5(b)], with very little quadratic chirp [Fig. 5(c)]. This particular FROG measurement is recorded with as little as 200 nJ of input UV energy. By changing the wavelength of the visible pulse, using the procedure described above, and changing the angle of the doubling crystal, we are able to change the wavelength. The FROG measurement of compressed pulses centered at 314 nm is shown in Fig. 6(a) and corresponds to a pulse duration of 42 fs [Fig. 6(b)] with a small quadratic chirp that is due to the prism compressor [Fig. 6(c)].

The system described above is reasonably stable and reproducible on a day-to-day basis, although we find that the poor mode quality of the pump can significantly degrade the performance of the OPA. Once aligned, it produces short pulses of the same wavelength, pulse duration, and chirp for several hours with peak-to-peak energy fluctuations in the UV of not more than 20%.

A significant advantage of type II phase matching is the possibility of separating the signal and the idler waves by polarization. This gives the ability to extend the IR tunability of the system. By placing a 1-mm-thick $AgGaS_2$ crystal directly after the OPA and blocking the 790-nm light with a 2-mm-thick Ge filter, we are able to generate as much as 0.5 μJ of tunable mid-IR radiation by difference-frequency mixing of the signal and the idler. This is a factor-of-10 improvement with respect to previously reported results.[2] We have not yet performed any spectral measurements (the center wavelength was calculated by use of the center wavelengths of the signal and the idler that were used for difference-frequency generation) or pulse duration measurements, but from the crystal data (see, for example, Ref. 2) we should expect sub-100-fs pulses in this wavelength range. Additional optimization, such as adding a delay line between these two waves, should result in higher conversion efficiencies, and using a thinner crystal should result in pulse durations of 50 fs or shorter.

We note that other nonlinear processes (some of them are shown in Fig. 7) can be used to generate all the possible colors of ultrashort pulses in the range from 12 μm to 280 nm. Compression of these pulses can deliver tunable, nearly transform-limited ultrashort pulses over the wide wavelength range of interest to most physicists, chemists, and biologists.

In summary, we have described a practical approach to generating nearly transform-limited ultrashort pulses tunable through the mid-IR, IR, visible, and UV ranges. Frequency-resolved optical gating is shown to be a helpful tool for characterizing and optimally compressing these pulses.

REFERENCES

1. M. Nisoli, S. De Silvestri, V. Magni, O. Svelto, R. Danielius, A. Piskarskas, G. Valulis, and A. Varanavicius, "Highly efficient parametric conversion of femtosecond Ti:sapphire laser pulses at 1 kHz," Opt. Lett. **19**, 1973–1975 (1994).
2. F. Seifert, V. Petrov, and M. Woerner, "Solid-state laser system for generation of midinfrared femtosecond pulses tunable from 3.3 to 10 μm," Opt. Lett. **19**, 2009–2011 (1994).
3. V. V. Yakovlev, B. Kohler, and K. R. Wilson, "Broadly tunable 30-fs pulses produced by optical parametric amplification," Opt. Lett. **19**, 2000–2002 (1994).
4. M. K. Reed, M. S. Armas, M. K. Steiner-Shepard, and D. K. Negus, "30-fs pulses tunable across the visible with a 100-kHz Ti:sapphire regenerative amplifier," Opt. Lett. **20**, 605–607 (1995).
5. S. R. Greenfield and M. R. Wasielewski, "Near-transform-limited visible and near-IR femtosecond pulses from optical parametric amplification using Type II beta-barium borate," Opt. Lett. **20**, 1394–1396 (1995).
6. F. Salin, F. Estable, and F. Saviot, "Tunable femtosecond sources and optical parametric generators," in *Ultrafast Phenomena IX*, P. F. Barbara, W. H. Knox, G. A. Mourou, and A. H. Zewail, eds. (Springer-Verlag, New York, 1995), pp. 194–195.
7. T. S. Sosnowski, P. B. Stephens, and T. B. Norris, "Production of 30-fs pulses tunable through the visible spectral region by a new technique in optical parametric amplification," Opt. Lett. **21**, 140–142 (1996).
8. B. Kohler, V. V. Yakovlev, J. Che, J. L. Krause, M. Messina, K. R. Wilson, N. Schwentner, R. M. Whitnell, and Y. Yan, "Quantum control of wave packet evolution with tailored femtosecond pulses," Phys. Rev. Lett. **74**, 3360–3363 (1995).
9. R. Trebino and D. J. Kane "Using phase retrieval to measure and intensity and phase of ultrashort pulses—frequency-resolved optical gating," J. Opt. Soc. Am. A **10**, 1101–1111 (1993).
10. B. Kohler, V. V. Yakovlev, K. R. Wilson, J. Squier, K. W. DeLong, and R. Trebino, "Phase and intensity characterization of femtosecond pulses from a chirped-pulse amplifier

by frequency-resolved optical gating," Opt. Lett. **20**, 483–485 (1995).
11. S. A. Akhmanov, A. S. Chirkin, K. N. Drabovich, A. I. Kovrigin, R. V. Khokhlov, and A. P. Sukhorukov, "Nonstationary nonlinear optical effects and ultrashort light pulse formation," IEEE J. Quantum Electron. **QE-4**, 598–605 (1968).
12. R. Danielius, A. Piskarskas, A. Stabinis, G. P. Banfi, P. Di Tripani, and R. Righini, "Traveling-wave parametric generation of widely tunable, highly coherent femtosecond light pulses," J. Opt. Soc. Am. B **10**, 2222–2232 (1993).
13. J. V. Rudd, G. Korn, S. Kane, J. Squier, G. Mourou, and P. Bado, "Chirped-pulse amplification of 55-fs pulses at a 1-kHz repetition rate in Ti:Al_2O_3 regenerative amplifier," Opt. Lett. **18**, 2044–2046 (1993).